SUPPLEMENTARY DATA accompanying EMBO JOURNAL paper 2011

TITLE: THE CRYSTAL STRUCTURE OF YEAST CCT REVEALS INTRINSIC ASYMMETRY OF EUKARYOTIC CYTOSOLIC CHAPERONINS

Authors: Carien Dekker, S.Mark Roe, Elizabeth A. McCormack, Fabienne Beuron, Laurence H. Pearl & Keith R. Willison

CONTENTS

Supplementary Table I	Data collection statistics
Supplementary Table II	Signature residues per subunit and per domain
Supplementary Figure S1	Purification of CCT rabbit α-actin Plp2 complex
Supplementary Figure S2	Self-rotation function data
Supplementary Figure S3	Alignments of N-termini of yeast CCT subunits
Supplementary Figure S4	Differential occupancy of nucleotide pockets
Supplementary Figure S5	Residual density in CCT complex cavity
Supplementary Figure S6	Signature residues mapped onto CCT structure

Reference list for Supplementary Tables and Figure legends

Supplementary Table I

Data collection statistics

Beam line	SLS –X06SA (detector: PILATUS)
Wavelength	1.0001Å
Oscillation	0.5°
Crystal Mosaicity	0.22°
Spacegroup	P1
Unit cell dimensions	a=159.1Å b=162.5Å c=268.1Å α=85.2° β=81.1° γ=61.2°
# Reflections* (observed/unique)	392,007 / 209,755
Resolution limits (Å) (high res shell)	85 – 3.8 (4.0-3.8)
Completeness (high res shell)	91.6% (93.2%)
Mean(I/sigI) (high res shell)	8.41 (1.92)
Rsym (high res shell)	7.7% (39.2%)

Refinement Statistics**

R work	30.7%
R free	34.4%
Deviations	0.003 bonds/ 0.687 angles
Ramachandran plot	85.6% preferred 9.7% allowed 4.7% outliers
Residues in model (total in sequence)	Cct1 8-557 (559) Cct2 3-518 (527) Cct3 6-531 (534) Cct4 7-528 (528) Cct5 30-559 (562) Cct6 1-544 (546) Cct7 16-530 (550) Cct8 5-538 (568)

* as output by XDS integration and scaling programs [1]
** using PHENIX refinement software [2]

Supplementary Table II
Signature residues per subunit and per domain, with yeast CCT residue numbering

Subunit	Cct1	Cct2	Cct3	Cct4	Cct5	Cct6	Cct7	Cct8
Equa-torial	28 Gln	12 Glu 32 Leu	56 Val 77 Ser 131 Asp	89 Ala	78 Asp	28 Gly 36 Asn 42 Thr 54 Lys 72 Thr 77 Ala 116 Arg	21 Gln 113 Lys 114 Pro	52 Asn 57 Asn 126 Glu
Inter-mediate	198 Tyr	152 Asp 166 Leu 183 Arg 186 Gly	197 Glu			137 Lys 166 Leu	161 Cys	175 Glu 191 Pro
Apical	204 Asn 206 Leu 208 Ala 209 His 222 Tyr 274 Arg 311 Val 312 Glu 346 Gly 350 Phe 360 Glu	209 Asp 236 Thr 259 Ala 262 Glu 287 Arg 288 Gln 289 Leu 291 Tyr 294 Pro 295 Glu 307 Glu 308 His 310 Asp 311 Phe 313 Gly 357 Ser	203 Tyr 236 Arg 242 Arg 255 Gly 266 Glu 292 Pro 298 Glu	203 Thr 208 Glu 237 Ile 238 Gln 257 Tyr 266 Glu 283 Cys 291 Ser 292 Ile 293 Leu 294 Arg 295 Asp 296 Ala 315 Asp 317 Glu 334 Ala 339 Phe	323 Cys 325 Trp 330 Glu 332 Asn 340 Leu 341 Pro 345 Trp 347 Gly 348 Gly	195 Glu 197 Met 199 Met 201 His 217 His 218 Gly 220 Arg 223 Asp 243 Glu 259 Arg 284 Val 303 Pro 324 Asn 336 Ala	200 Gly 202 Lys 226 Tyr 228 Gly 229 Phe 247 Glu 253 Glu 257 Ala 258 Glu 275 Trp 295 Ser 297 Leu 304 Thr 313 Phe 315 Ala 316 Gly 363 Asn	234 Gly 263 Gly 266 Leu 292 Ala
Inter-mediate	398 Met	391 Leu	385 Ser 395 Asn 410 Pro			393 Asp 400 Arg	398 Met 399 Ile	402 Asp
Equa-torial	526 Lys	506 Glu	441 Pro 442 Tyr 486 Gly 512 Thr 528 Ser	484 Val 506 Ser	459 Asp 502 Gln 537 Gln 543 Gln	476 Glu 529 Leu	466 Asn 523 Thr	479 Tyr 543 Gln
TOTAL	**15**	**24**	**19**	**20**	**14**	**27**	**25**	**12**
TOTAL apical	**11**	**16**	**7**	**17**	**9**	**14**	**17**	**4**

Alignments were performed as described [3] using T-Coffee [4]

FIGURE LEGENDS SUPPLEMENTARY FIGURES

Supplementary Figure S1

Purification of CCT rabbit α-actin Plp2 complex. **A**. CCT (i.e. CCT-3CBP-ANC2) was ATP-treated to release remaining bound substrates [5,6], and purified using a Superose 6 gel filtration column. Shown are fractions 10-16 on a 12% SDS gel, with all eight CCT subunits running around the 60kDa mark. **B**. The pure and 'empty' CCT was then used to bind EDTA-unfolded α-actin in the presence of yeast Plp2 and purified again by gel filtration. Since α-actin is not released by yeast CCT [7], this leads to a stable ternary complex, as shown by the peak fractions on the gel. Note that, from the fraction numbers, the ternary complex runs at a slightly lower elution volume than empty CCT in panel **A**. **C**. Western blot analyses of different gel filtration runs, using anti-His antibody against His-tagged Plp2 [6]. Also, CBP-tagged CCT reacts due to the His sequence in the tag-linker [5]. The blot shows that Plp2-binding to CCT is stronger in the presence of α-actin, and supports the notion that the CCT-Plp2-α-actin complex forms a stable ternary complex. **D**. Multiple tiny crystals out of a total of 13 drops were transferred to a CoStar tube with 0.22μm filter, washed with well solution and dissolved in SDS sample buffer and analysed on a silverstained 10% SDS gel. The high PEG8k and glycerol content of both crystals and well solution results in a wavy appearance of the bands. The difference in intensity for the eight CCT bands and the actin and Plp2 bands reflects the mass ratio of 1:23 for one actin molecule binding to 16 CCT subunits. The presence of Plp2 was also confirmed by Western blot analysis. **E.** When loading 1/8th of the sample volume in **D**, the individual bands of CCT subunits become discernable. **F, G, H** illustrate typical 2Fo-Fc densities

within different subunits, which are characteristic of a 3.8Å density map, namely Cct6 (**F**), Cct2 (**G**) and Cct8 (**H**).

Supplementary Figure S2

Self-rotation function data. **A**. Self-rotation plot at Chi = 180 for CCT data as calculated by Molrep (CCP4[8]) using data from 8-15Å and a radius of 50Å. The strongest peak arises from the 2-fold axis relating the two molecules to each other (RF=10.6). The next two highest peaks are significantly stronger than all other remaining peaks (RF=8.4 and 6.6 as compared with RF<=5.2), and indicate the presence of two proper 2-fold axes as opposed to the remaining pseudo 2-fold axes. The position of these two stronger peaks is consistent with the orientation of the Cct4-Cct6 axes of the two molecules relative to each other in the unit cell. **B**. Self-rotation plot for the theoretical case of α-CPN in the same unit cell as CCT, showing eight equivalent proper 2-fold axes per molecule, due to eight identical subunits per ring. **C**. Schematic representation of the two molecules in the P1 unit cell with, for each case a proper 2-fold axis going through a plane disecting Cct4-Cct6.

Supplementary Figure S3

A. Alignments of N-termini of the eight yeast Cct subunits. **B**. Alignments of the N-termini of yeast, worm, mouse and human CCT5 subunits.

Supplementary Figure S4

Differential nucleotide occupancy of the nucleotide pockets illustrated for subunit Cct2 where an ADP-BeF molecule was modelled (**A**) and subunit Cct4 where a sulphate ion was modelled (**B**). Density of the (2Fo-Fc) map is shown at 1.2 sigma.

Supplementary Figure S5

A. CCT, shown as the entire complex, and **B**. as a slice through the complex with ncs-averaged density superposed (see CCT actin section in manuscript and legend to Figure 4A) to highlight the asymmetric distribution of residual density, both with respect to the cavity and to the entire complex. The lower cavity reveals some density, but it is not as substantial and contiguous as in the upper cavity. Furthermore, the density in the lower cavity has no discernable protein features, like β-strands, unlike the density in the upper cavity.

Supplementary Figure S6

A-**B**. Signature residues [3] mapped onto the structure of the CCT complex (apical domains only) in its closed conformation. **A** is the view from the outside of the complex, possibly indicating residues involved in co-factor binding. **B** is the view from inside the cavity, showing residues possibly involved with substrate interaction. **C.** Consensus sequence based on an alignment of all eight yeast CCT subunits mapped onto the 3D structure of a single CCT chain, with fully conserved residues in red, conserved substitutions in orange and semi-conserved substitutions in green. Nucleotide is shown in yellow. **C-K**. Signature residues for each Cct subunit mapped onto its structure. Shown in red are the residues that are fully conserved amongst orthologues with no identity score amongst paralogues. All figures were produced in Pymol[9].

References for Supplementary Tables I, II and Legends to Supplementary Figures 1-6

1. Kabsch, W. Automatic-Indexing of Rotation Diffraction Patterns. Journal of Applied Crystallography 21, 67-71 (1988).
2. Adams, P. D. et al. PHENIX: building new software for automated crystallographic structure determination. Acta Cryst. D58, 1948-1954 (2002).

3. Pappenberger, G. et al. Crystal structure of the CCT gamma apical domain: Implications for substrate binding to the eukaryotic cytosolic chaperonin. Journal of Molecular Biology 318, 1367-1379 (2002).
4. Notredame, C., Higgins, D. G. & Heringa, J. T-Coffee: A novel method for fast and accurate multiple sequence alignment. Journal of Molecular Biology 302, 205-217 (2000).
5. Pappenberger, G., McCormack, E. A. & Willison, K. R. Quantitative actin folding reactions using yeast CCT purified via an internal tag in the CCT3/gamma subunit. Journal of Molecular Biology 360, 484-496 (2006).
6. McCormack, E. A., Altschuler, G. M., Dekker, C., Filmore, H. & Willison, K. R. Yeast phosducin-like protein 2 acts as a stimulatory co-factor for the folding of actin by the chaperonin CCT via a ternary complex. Journal of Molecular Biology 391, 192-206 (2009).
7. Altschuler, G. M. et al. A single amino acid residue is responsible for species-specific incompatibility between CCT and alpha-actin. Febs Letters 583, 782-786 (2009).
8. CCP4. Collaborative Computational Project No. 4: The CCP4 suite: programs for protein crystallography. Acta Cryst. D50, 760-763 (1994).
9. DeLano, W. L. The PyMOL Molecular Graphics System. DeLano Scientific, San Carlos, CA, USA, http://www.pymol.org. (2002).

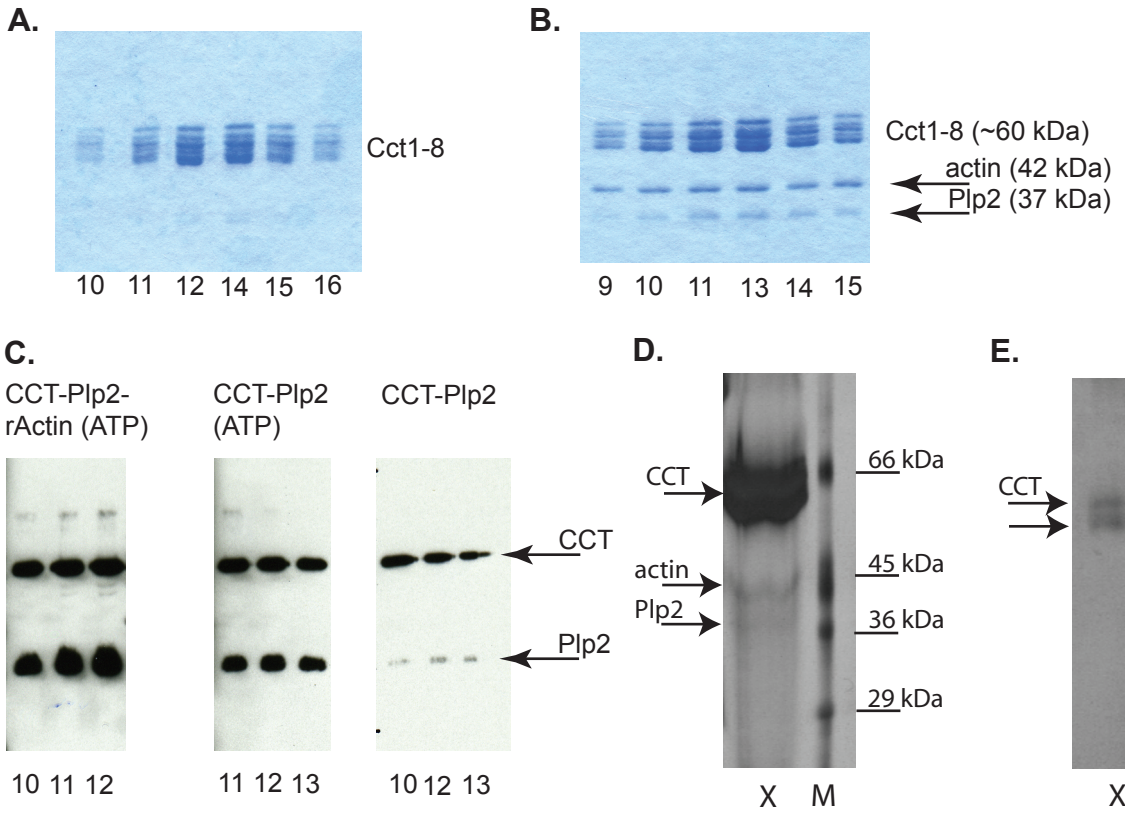

Supplementary Figure S1.

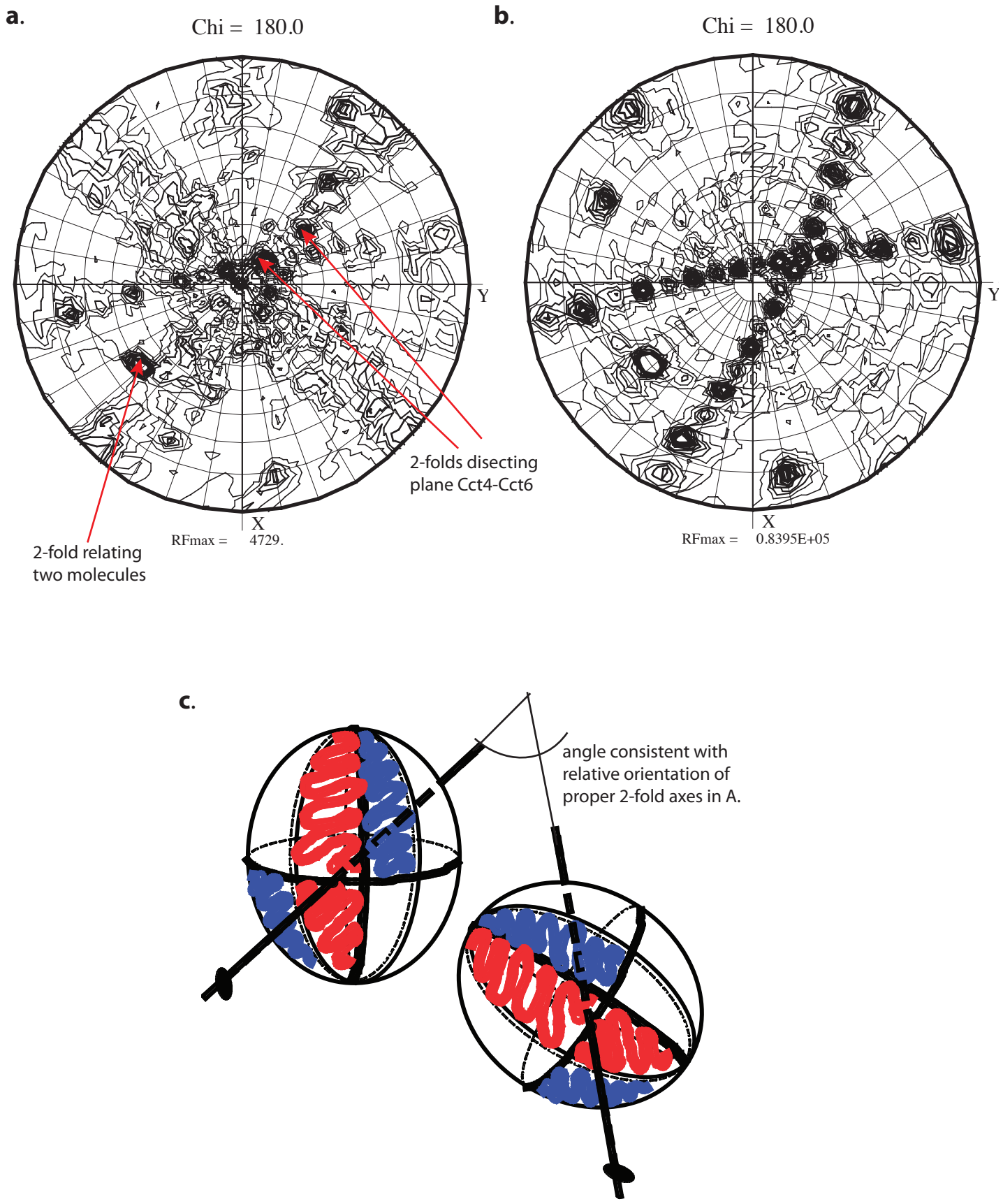

Supplementary Figure S2.

A.

```
Sc-CCT1 ------------------------- MSQLFNNSRSDTLFLGG --EKISGDDIRNQN VLATMAVANVVK SSLGP
Sc-CCT2 ------------------------- MSVQIFGDQV -----TE--ER--AENARLSA FVGAIAVGDLVK STLGP
Sc-CCT3 ---------MQAPV----------------- VFMNA------ S-QERTTGRQAQISN ITAAKAVADVIR TCLGP
Sc-CCT4 ---------MSAK----------------- VPSNAT------ F-KNKEKPQEVRKAN IIAARSVADAIR TSLGP
Sc-CCT5 MAARPQQPP MEMPDLSNAIVAQDEMGRPFIIVKDQG ------N-KKRQHGLEAKKSH ILAARSVASIIK TSLGP
Sc-CCT6 ------------------------- MSLQLLNPK --------- AESLRRDAALKVN VTSAEGLQSVLE TNLGP
Sc-CCT7 ------------------------- MNFGSQTPTIVVLKEG -TDASQGKGQIISN INACVAVQEALK PTLGP
Sc-CCT8 ------------------------- MSLRLPQNPNAGLFKQGYN SYSNADGQIIKS IAAIRELHQMCL TSMGP
```

B.

```
SACEREV MAARPQQPPMEMPDLSNAI VAQDEMGRPFIIVKDQGNKKRQHGLEAKKSHILAARSVASIIKTSLGP
CAENELE ----------MAQSSAQLLFDESGQPFIVMREQENQKRITGVEAVKSHILAARAVANTLRTSLGP
MUSMUSC ---------- MASVGTLAFDEYGRPFLIIKDQDRKSRLMGLEALKSHIMAAKAVANTMRTSLGP
HOMOSAP ---------- MASMGTLAFDEYGRPFLIIKDQDRKSRLMGLEALKSHIMAAKAVANTMRTSLGP
```

Supplementary Figure S3.

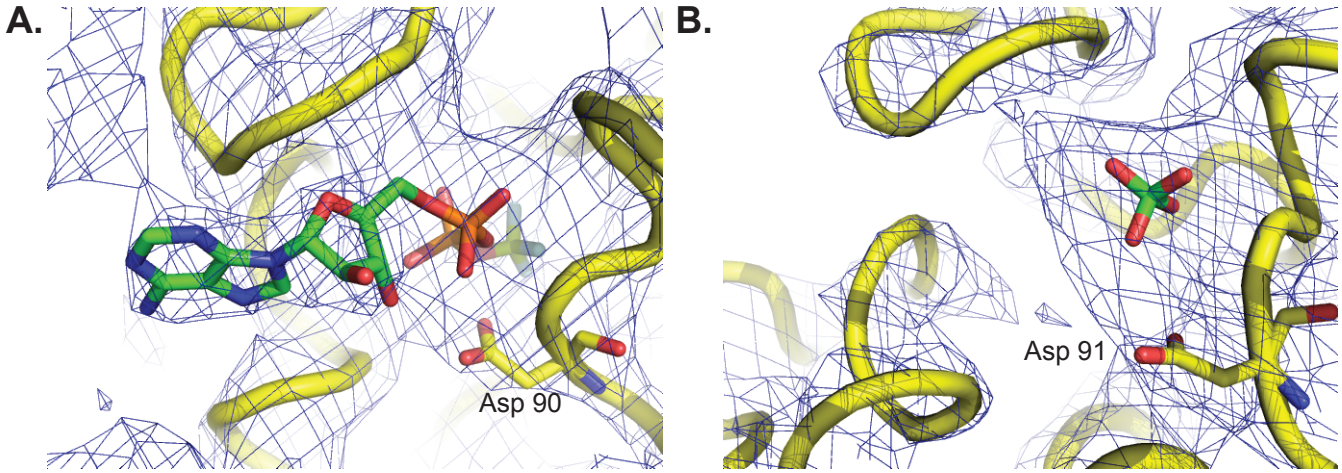

Suppl Figure S4.

A.

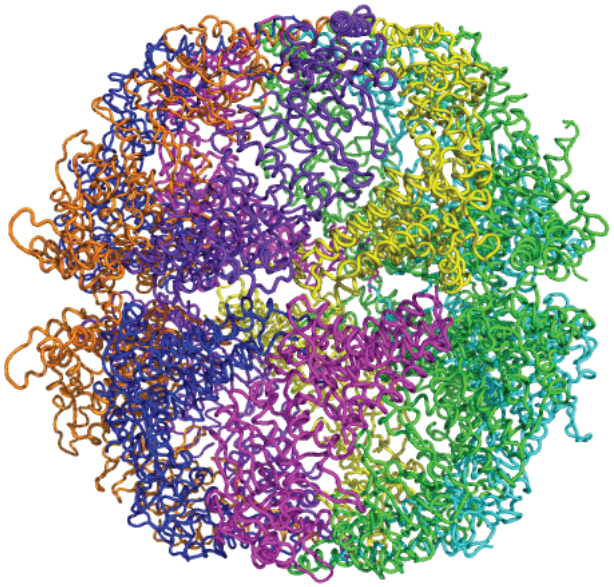

B.

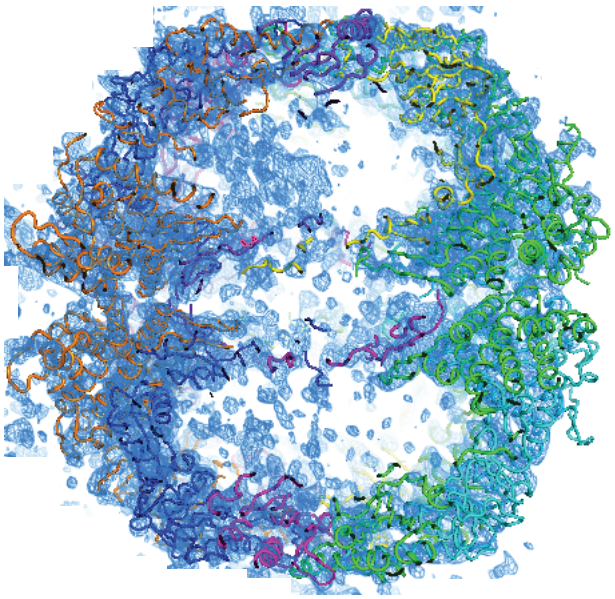

Supp Figure S5.

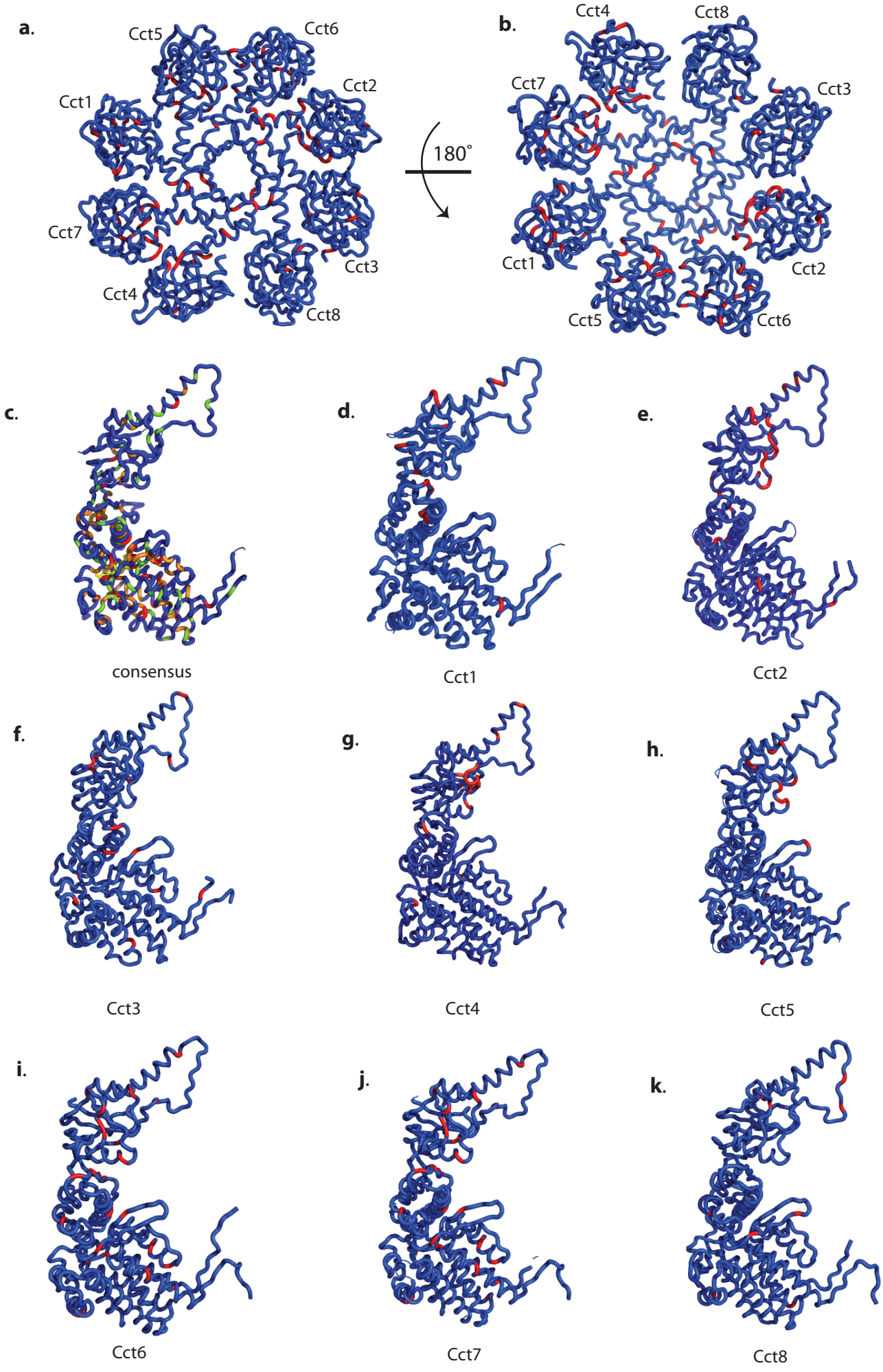

Supplementary Figure S6.